WHITE PAPER

Dosimetry for Yttrium-90 Microsphere Brachytherapy

Aaron Nelson, MD, Amy Swallen, Matt Arpidone, Sydney Lindner, and Dennis Nelson, PhD
MIM Software Inc.

Introduction

Yttrium-90 (^{90}Y) microsphere brachytherapy for liver cancer is a type of selective internal radiation therapy that delivers radiation from microspheres that have become lodged in small vessels after injection through the hepatic artery. ^{90}Y microsphere therapies take advantage of the unique blood supply to the liver whereby tumors receive 80-100% of their blood supply from the hepatic artery compared to normal liver tissue which receives only 20-30% of its blood supply from the hepatic artery.

^{90}Y is a beta emitter with a range slightly less than 4 mm in water for the average energy beta particle, while the range of the maximum energy ^{90}Y beta is 11 mm. Ninety percent of the emitted energy is absorbed within a radius of 5.3 mm.[1] ^{90}Y microspheres deliver dose as a permanent brachytherapy implant to the local tissue and cause embolization of the vessel feeding tumor cells.

Currently, there are two commercially available ^{90}Y-microsphere products and each type, resin or glass, has a slightly different recommended method for planned dose. It is recommended that when using resin spheres, an administration of 2.0-3.0 GBq of activity be injected depending on the percent of tumor involvement in the liver.[2] If the liver-lung shunt is greater than 10% then a reduction in the injected dose with resin spheres is required.[2] The liver-lung shunt percentage is calculated from planar or SPECT Tc99m MAA exams after injecting the tracer into a similar arterial location as will be used for therapy delivery. The formula for liver-lung shunt is below:

$$\%\,Shunt = \frac{Lung\ Counts}{Liver\ Counts + Lung\ Counts} * 100$$

For therapy using glass spheres, a dose to the liver of 80 Gy to 150 Gy is recommended.[3] The formula used to calculate liver dose is

$$Dose(Gy) = 50 * \frac{Injected\ Activity * (1 - F)}{Liver\ Mass}$$

where the liver mass is derived from the volume of the liver and liver density and F is derived from the % Shunt formula above and represents the fraction of injected radioactivity localizing in the lungs.[3,4]

Both of these dosimetry models assume uniform dosimetry throughout the targeted areas of the liver and do not give information about the actual distribution of microspheres in tumors or in normal tissue. Additionally, the treatment delivered can differ from what was planned due to differences in catheter placement and delivery.

It has been discovered that the distribution of microspheres after injection can be evaluated through the use of post-treatment images from PET[5] and SPECT[6] for personalized post-treatment dosimetry calculations.[7]

Several voxel-based dosimetry models have been developed that utilize the activity concentrations from post-treatment imaging including the local deposition model (LDM),[8] dose point kernel convolution (DPK),[4] voxel S value (VSV) kernel convolution,[4] collapsed cone convolution,[9] and Monte Carlo dose calculation.[10,11] Both LDM and VSV methods have been implemented in MIM SurePlan™ and will be discussed in greater detail in the following sections on dosimetry.

Post Treatment Imaging with ^{90}Y

Both PET and SPECT have been used to evaluate the post-injection distribution of microspheres. While ^{90}Y is not an ideal PET imaging agent, there is a positron produced during ^{90}Y beta decay at a rate of 1 out of every 31,387 disintegrations that can be used to generate a PET image.[12] In terms of SPECT imaging, ^{90}Y lacks discrete-energy photon emissions, such as gamma rays, however, the Bremsstrahlung photons which are produced from interactions of the beta particles with soft tissue can be imaged with SPECT.[6] Quantitatively accurate PET and SPECT image reconstructions are important since the accuracy of dose calculation is highly dependent on the accuracy of the image's activity concentration.

Quantitative Imaging with ^{90}Y PET

The possibility of quantifying the distribution of ^{90}Y using PET was demonstrated by Nickels et al. in 2004.[10] Despite a relatively low yield of positrons and a high random fraction from Bremsstrahlung radiation and photons generated by the natural ^{176}Lu present in the crystals, studies have shown that quantitatively accurate activity distributions can be measured with the potential for deriving accurate dosimetric data.[7,13]

In 2015 Willowson and The QUEST Phantom Study group performed a large multi-institutional study to look at the quantitative accuracy of ^{90}Y imaging for different PET/CT scanners from GE, Philips, and Siemens for the purpose of dosimetry after radioembolization.[14] They tested 69 PET/CT scanners, 37 with time-of-flight (ToF) and resolution recovery (RR) capability, from a total of 47 centers from 13 countries.

Their findings demonstrated that total activity and background activity could be measured to within 10% of true values. The hot spheres > 20 mm in size had a measured activity within 20% of the true value while spheres < 20 mm in size demonstrated typical partial volume effects. These findings agree with other recent studies where spheres > 20 mm in size were underestimated by approximately 5 to 20%.[14-17] The QUEST authors concluded that they were able to achieve acceptable performance for measuring activity concentrations over a range of clinically realistic activity concentrations (50-300 kBq/ml).

In 2015 Carlier et al. also evaluated the quantitative accuracy of ^{90}Y in 32 patient images.[15] In their study they found a goodness of fit of 1.00 between the measured and expected activity for the whole field of view and a goodness of fit of 0.89 for the liver with an approximately 16% activity underestimation. The authors felt the small difference for the liver was an acceptable result and was largely due to not accounting for the lung shunt fraction or residual activity in the tubing as well as the uncertainty in the

Reconstruction Parameters Found to be Most Accurate from the QUEST Trial*

Vendor	Model	Recommended reconstruction for quantitative purposes	Error in warm background concentration measures (%)		Error in 37-mm hot sphere concentration measures (%)	
			Average±SD	Range	Average±SD	Range
GE Healthcare	Discovery 690, 710	3D OSEM with all-pass filter: e.g., 2i24s + RR + ToF	1±4	+6 – 7	-14±9	-5 – 28
Philips	Gemini TF	3D OSEM (BLOB OS TF) with no filter: 4i8s + ToF	-5±2	-4 – 6	-22±3	-20 – 24
Siemens	Biograph mCT	3D OSEM with all-pass filter: 2i21s + RR + ToF	-2±6	+4 – 9	-16±4	-13 – 22

Results are from day 0 imaging with a hot sphere concentration of 2500 kBq/ml and a warm phantom background concentration of 300 kBq/ml.

**Sites were encouraged to use reconstruction parameters that had proven successful in their own ^{90}Y experience, with all available corrections (scatter, attenuation, random coincidences, ToF, and RR where available).*

dose calibration of the expected activity. In another patient study evaluating quantitative accuracy,[18] Marti-Climent et al. evaluated 10 patients treated with ^{90}Y microspheres and also reported good agreement between measured and expected activity in the liver with an average difference of 10%. In this study the authors did take into account the lung shunt as determined by planar scintigraphy.

Quantitative Imaging with ^{90}Y Bremsstrahlung SPECT

Unlike many radionuclides used in nuclear medicine, ^{90}Y lacks discrete-photon emissions, such as gamma rays and characteristic x-rays. The gamma rays and x-rays that are produced are both low in quantity (<<1 ppm) and are not in a useful energy range for imaging (~2 MeV and <<18 keV respectively).

The activity distribution of ^{90}Y can be imaged using SPECT, however, through Bremsstrahlung photons produced by the interactions of the beta particles with tissues. A continuous energy spectrum is produced and can be expressed as the sum of 5 components: primary Bremsstrahlung, object scatter, camera backscatter, collimator scatter and penetration, and lead x-rays produced in the collimator.[6] While the lack of a photopeak has made imaging with ^{90}Y more difficult, a number of methods have been developed to produce more quantitative information.

Monte Carlo methods which model the energy dependent object attenuation, scatter, and collimator detector response have been developed.[19] Rong et al. developed a Monte Carlo method accounting for these factors and demonstrated good accuracy with errors of only 5-10% compared to known activity using physical and synthetic phantoms.[19] Elshot et al. directly incorporated Monte Carlo simulations of energy dependent scatter and attenuation into the reconstruction algorithm.[20] Dewarja et al. also developed a Monte Carlo based scatter estimation method using the patient's SPECT/CT images as input to the simulator and found errors for 80-ml and 40-ml lesions were decreased from 29% and 38% without scatter correction to 1% and 12% with the Monte Carlo scatter correction.[21] While Monte Carlo methods have produced good results, they are not widely available in clinics.

More recently a method was developed by Siman et al. that can be applied to commercial SPECT/CT systems and used in other clinics.[6] Their method involved determining an appropriate imaging energy window, as well as its energy window-based background compensation, and applying CT attenuation correction. They showed how SPECT reconstruction parameters can be optimized and when combined with self-calibration can produce quantitative activity distributions from SPECT images.

Imaging was performed by Siman et al. using a Siemens Symbia TruePoint SPECT/CT with a Medium Energy Low Penetration (MELP) collimator. Projection images were obtained at 28 seconds per projection with 2x64 projections over 360 degrees. Images were acquired with a 128x128 matrix and a 4.8 mm voxel size. An imaging energy window (90-125 keV) and a background compensation energy window (310-410 keV) were used. A scaling factor of 0.53 was applied to the background compensation energy window. CT-based attenuation correction was performed using a bilinear fit curve with a mean energy of 107 keV. Using these parameters, they were able to improve the recovery coefficient of a 37 mm sphere from 37% to 90% (in a 10 mm volume of interest) and decreased the residual activity in a lung insert from 44% to 14%. The authors concluded that the method they developed could be employed by other clinics to result in more quantitatively accurate SPECT images.

Image Correction — PET Cameras That Do Not Include ^{90}Y as an Option for Reconstruction

The post-^{90}Y PET image provides the measured activity in each voxel after having been decay corrected over the time of the scan, typically to either the time of acquisition or time of injection, and corrected for the branching fractions by the PET reconstruction software using the selected acquisition isotope. At this time, most PET scanners do not have ^{90}Y available as an isotope to select for image reconstruction. Therefore, prior to dose calculation the PET data

must be corrected from the isotope selected for image reconstruction to the isotope that was actually injected, ^{90}Y. It is important to note that ^{90}Y is still used as the injected isotope even if another isotope (e.g., ^{22}Na) had to be selected in the reconstruction software. SurePlan will undo the decay factor and branching factor corrections of the selected isotope for reconstruction and then apply the appropriate factors for ^{90}Y.

Initial steps to undo any processing completed by the PET scanner are done using the DecayFactor (0054,1321) and DecayCorrection (0054,1102) DICOM tags. The DecayFactor tag gives the factor that the image values were multiplied by to correct to the time provided in the DecayCorrection tag, which has set options of NONE, START (i.e., Acquisition Start Time), or ADMIN (i.e., Injection Time entered by Physician). If the DecayFactor tag is missing or the image needs additional corrections to time of injection, correction factors are computed and applied to the image voxels that account for incorrect decay and branching factors applied during reconstruction. There are two decay correction factors when DecayCorrection = START and three decay correction factors when DecayCorrection = ADMIN which are applied during reconstruction. The applied decay corrections and a branching factor which are isotope specific must be corrected prior to dose measurement. Since ^{90}Y microspheres are a permanent implant, it is reasonable to assume that all isotope decay occurs at the same location for each microsphere. A(t) is isotope activity as a function of time, A0 is the PET activity level at the beginning of image acquisition, and λ is the decay constant of the isotope based on its half-life:

$$A(t) = A_0 e^{-\lambda t}$$

The correction factor for isotope decay, IDF, during an image's acquisition is:

$$IDF(\lambda) = \lambda t / (1-e^{-\lambda t})$$

The correction factor to account for difference in isotope decay during image acquisition between the isotope used for acquisition, ACQ, and ^{90}Y is:

$$C_{IDF} = IDF(\lambda_{90Y})/IDF(\lambda_{ACQ})$$

Reconstruction also accounts for delay between when scanning is started and the start of imaging for each image slice position. When time from scan start to time of image slice acquisition is T_{ItoS}:

$$C_{ItoS} = e^{\lambda_{90Y} T_{ItoS}} / e^{\lambda_{ACQ} T_{ItoS}}$$

The branching fraction must be corrected by using the ratio of the branching fraction of the acquisition isotope (B_{ACQ}) to the branching fraction of ^{90}Y (B_{Y90}):

$$C_{BF} = B_{ACQ}/B_{90Y}$$

The image correction factor, CF, which corrects for isotope decay and branching fraction for an image that has been reconstructed using an isotope other than ^{90}Y, is:

$$CF = C_{IDF} * C_{ItoS} * C_{BF}$$

Dose measurements require activity levels present at isotope injection. When DecayCorrection (0054,1102) = START then correction from isotope injection to time of PET scanning for time difference is CF_{Delay}

$$CF_{Delay} = e^{\lambda_{90Y} * T_{Delay}}$$

When DecayCorrection (0054,1102) = ADMIN then

$$CF_{Delay} = e^{\lambda_{90Y} * T_{Delay}} / e^{\lambda_{ACQ} * T_{Delay}}$$

since the image has been corrected previously for decay of the acquisition isotope.

The final Image Correction factor, ICF, that is multiplied by all image voxels:

$$ICF = CF * CF_{Delay}$$

Image Correction — Scaling to Known Injected Activity

Rather than correct the native PET values back to time of injection using decay corrections, this method uses the distribution of activity in either PET or SPECT and scales that distribution so that the total activity in the image matches the measured, injected activity as input by the user. First, all of the values in the self-calibration region, or the volume containing the total injected activity, are summed:

$$A_{Total} = \sum A_{Vox}$$

where A_{Total} is the total sum of activity y in the self-calibration region and Avox is the activity in each voxel x. Each voxel is divided by this total to give a normalized voxel value that is a percentage of the total (N_X).

$$N_x = A_{Vox} / A_{Total}$$

This normalized voxel value is multiplied by the total injected activity (A_{INJ}) in GBq as input by the user from their pre-injection measurements and divided by the volume of the voxel (V_X) in ml to give each voxel a unit of Bq/ml.

$$N_{INJ} = N_x * A_{INJ} / V_x$$

where N_{INJ} is the normalized activity injected into each voxel. This activity is then multiplied by the local deposition dose model constant to get a final dose per voxel.

Dose Calculation Models

Three dose calculation models are available in SurePlan: Voxel S Value approach based on MIRD Pamphlet 17, Local Deposition Model, and Local Deposition Model with Known Activity. All three methods are available for PET, however, only LDM with Known Activity is available for SPECT images that are not in Becquerels per milliliter (Bq/ml).

Voxel S Value (VSV) Dose Calculation

The voxel S value convolution (VSV) method in SurePlan is an approach based on the ^{90}Y schema defined in MIRD Pamphlet 17 for non-uniform distribution of radioactivity.[4] The 3x3x3 mm VSV kernel for ^{90}Y is convolved with the PET activity concentration image (in Bq/ml), that has been decay corrected back to the time of injection, to calculate the absorbed dose in units of Gy.

MIRD Pamphlet 17 has applied Monte Carlo methods for ^{90}Y sources in water to calculate dose deposited in 3x3x3 mm target voxels surrounding a uniform source of Y^{90} in the central voxel. The MIRD matrix is a matrix of voxel S values. The calculated dose includes energy deposited from the predominant Beta minus emissions and also dose due to Bremsstrahlung radiation. Since only one positron is emitted for every 31,387 Beta minus emissions[12] the dose due to positrons is not calculated. Due to finite PET image resolution, the VSV assumption of uniform activity in the source voxel is preferred for dose calculations.

Rather than creating a new Monte Carlo kernel for the voxel size of each image, the PET image is resampled to 3x3x3 mm voxels using trilinear interpolation. Trilinear interpolation is a commonly used method of approximating the value at a 3D coordinate located within a regular 3D grid of data points. For a 3D image with intensity value I(u,v,w) for the voxel located at the position (u,v,w), where u,v,w are integral numbers, the value T(x,y,z) represents the trilinear interpolated value at the position (x,y,z) where x,y,z are real numbers.

$$T(x,y,z) = \sum_{i=0}^{1}\sum_{j=0}^{1}\sum_{k=0}^{1}\begin{bmatrix} I(\lfloor x\rfloor + i, \lfloor y\rfloor + j, \lfloor z\rfloor + k) \\ \cdot (1 - |\lfloor x\rfloor + i - x|) \\ \cdot (1 - |\lfloor y\rfloor + j - y|) \\ \cdot (1 - |\lfloor z\rfloor + k - z|) \end{bmatrix}$$

The intensity value at (x,y,z) is approximated by taking each of the eight closest data points and multiplying its intensity value by a weight that is based on the distance in each dimension from (x,y,z), then summing

the weighted intensity values. In each dimension, the weighting provides a linear transition from the data on one side of the coordinate to the data on the other side of the coordinate.

Image resampling in MIM is performed using trilinear interpolation. A new voxel grid is established at the requested resolution, with dimensions that allow the entire original image to be enclosed within. The intensity value at each new voxel grid location is then computed by performing trilinear interpolation at the corresponding location in the original image.

When the resampling resolution is lower than the image resolution, considering only the eight voxels of the original image that are closest to the interpolation point may result in some of the original data not being taken into account. Consider the case of resampling from 1 mm to 3 mm in a single dimension:

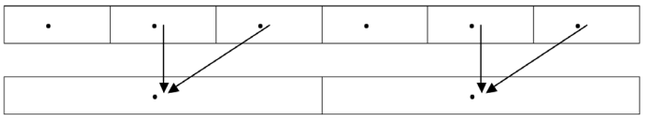

The upper row represents the input data with 1 mm spacing, while the bottom row represents the output data with 3 mm spacing. The arrows represent the input data points being used in the computation of each output data point. Because only the two closest points are used, every third point of the input data is effectively ignored. To avoid this issue, MIM uses a hierarchical downsampling process. Additional intermediate interpolation steps are added to ensure that all of the input data is considered. The input spacing is doubled repeatedly, and an interpolation step performed at that doubled spacing, until the spacing is greater than half the desired output spacing. Because the spacing increases by no more than a factor of two between each level, the resampling operation at each level will not disregard any input data from the previous level. The end result is that the final image contains a contribution from every input voxel.

For the process of resampling from 1 mm to 3 mm, an additional 2 mm resolution level is introduced. This results in an overall sampling scheme that looks like this:

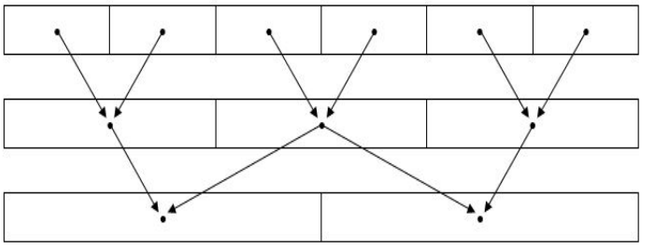

For more information on trilinear interpolation:
"Mathworks Documentation: interp3" https://www.mathworks.com/help/matlab/ref/interp3.html
or
Press, WH. "Chapter 3: Interpolation and Extrapolation." Numerical recipes in C: the art of scientific computing. Cambridge University Press 1988. 123-128.

Local Deposition Model (LDM) Dose Calculation

The Local Deposition Model assumes that the measured activity in a voxel is proportional to the energy deposited in that voxel. Absorbed dose is calculated for LDM by multiplying the measured activity concentration in each voxel (Bq/ml) by a constant scalar factor (Gy/Bq/ml) to convert the activity concentration image to dose in Gy.[8,22,23]

Due to the finite resolution of PET, the true activity distribution is blurred by the point spread function of the imaging modality. Therefore, the measured activity in a voxel is not solely from the actual activity in that voxel but is rather the result of a convolution of a Gaussian, which defines the camera system resolution, with all point sources both within the voxel of interest and surrounding voxels. If we assume the spread of energy deposition from a ^{90}Y point source of activity can be modeled as a Gaussian, then the net energy accumulated at a point is proportional to the convolution of a Gaussian with all point sources. This results in a similar blurring of energy deposition

as is seen with the blurring of the measured activity. The LDM method relies upon the spread of activity reflecting the spread of the energy deposition. When the PET system resolution is nearly equal to the energy deposition profile from a point source, the LDM method has the most accuracy in providing a measure of energy deposition in a given voxel, since the accumulation of activity and energy deposition will be similar for that voxel.

In order to determine the PET camera resolution that best defines energy deposition in a voxel, a simulated phantom of spherical sources was convolved with 3x3x3 mm voxel S values for ^{90}Y as reported in MIRD Pamphlet 17 Table B3.[4] This table contains the 3 mm voxel dose distribution matrix for ^{90}Y in water for a distance up to 18.75 cm from the source voxel. The central voxel is assumed to have a uniform distribution of ^{90}Y. The % decrease in S value for every 3 mm increment from the center of the source voxel is 83%, 92%, and 94% for a net decrease to 0.08% of the original value at 9 mm from the source voxel. The range of the maximum energy ^{90}Y Beta minus particle is 11 mm and the range of the mean energy ^{90}Y Beta minus particle is slightly less than 4 mm.[8] Since distance from the source is included in the convolution, the effect of absorbed dose fraction, which defines the fraction of dose absorbed at a given distance from a point source, is included in the convolution. The effect of the PET system resolution on the ^{90}Y dose is seen in the section below titled "LDM ^{90}Y Dose Relative to PET System Resolution."

Derivation of the LDM Constant

The LDM constant is derived by taking the average energy released per decay (Eavg) of ^{90}Y based on the probability density function Ψ(E) for emission:

$$E_{avg} = \int_0^\infty E * \psi(E) dE = 0.935 MeV = 1.498 * 10^{-13} J$$

Using the average energy, the total energy deposited ($E_{deposited}$) per unit volume over the entire isotope decay (t) is found using:

$$E_{deposited} = A_{INJ} E_{avg} \int_0 e^{-\lambda_{ACQ} t}\, dt = \frac{A_{INJ} E_{avg}}{\lambda_{ACQ}}$$

where t is assumed to be infinity due to the permanent implant of microspheres, A_{INJ} is the activity at time of injection and λ_{ACQ} is the ^{90}Y decay constant based on a half life of 64.1 hours. Total absorbed dose takes into account the density of liver (ρ) in kg/ml where liver density is 1.04 /1000 kg/ml.

$$D = \frac{A_{INJ} E_{avg}}{\lambda_{ACQ} * \rho_{liver}}$$

$$D = A_{INJ} * \frac{1.498 * 10^{-13}(J)}{3 * 10^{-6}(s^{-1}) * \frac{1.04}{1000}(\frac{kg}{mL})}$$

$$D = A_{INJ} * 4.794 * 10^{-5}(Gy * \frac{mL}{Bq})$$

Since the injected activity is the only unknown variable, the voxel activity is multiplied by the constant 4.794*10^{-5} Gy/Bq/ml to convert to absorbed dose.[8]

Bremsstrahlung radiation is not accounted for with the LDM method and is assumed to be negligible.[10] It has been shown that the Bremsstrahlung dose for a point source of ^{90}Y in a water medium is 0.001 of the Beta minus dose for all distances up to 3 mm from the source.[24] While not accounting for Bremsstrahlung radiation, the LDM method has been found to agree well with methods that do account for Bremsstrahlung radiation including VSV[8] and Monte Carlo methods. In particular, the SurePlan LDM dose calculation method was found to be within 2.5% of a Monte Carlo dose calculation technique for mean tumor and liver dose with greater than 0.99 linear correlation when evaluated on 31 clinical patients.* **Data on file*

LDM Dose Measurement with Known Activity

^{90}Y PET images and ^{90}Y Bremsstrahlung SPECT

images that have count levels proportional to actual ^{90}Y activity concentrations can be used for dose measurement using "LDM with Known Activity." The "known activity" refers to the known injected microsphere radioactivity in GBq (gigabecquerel) or mCi (millicuries). This method assumes that all of the injected microspheres are included in the field of view of the PET or SPECT image. A scalar is calculated as the ratio of the total injected activity, Bq, to the total measured counts in the self-calibration region. Multiplication of each voxel (counts) by this scalar (Bq/counts) converts the image to units of Bq for each voxel. The radioactivity per ml at any voxel is calculated as the Bq of that voxel divided by the voxel volume, ml. This scaled image now has units of Bq/ml and the LDM dose measurement method constant, $4.794 * 10^{-5}$ Gy/Bq/ml, can be used to convert the image to absorbed dose in Gy. The effects of PET or SPECT image resolution on absorbed dose calculations for LDM with Known Activity are identical to the LDM method.[23]

The self-calibration region chosen to include the total injected activity can have a significant impact on the dose calculation results. In 2018, Balagopal and Kappadath investigated absorbed dose results when using five different SPECT self-calibration regions for the LDM with Known Activity calculation. When comparing using the entire SPECT field of view versus a chest-abdomen contour as the self-calibration region, resulting mean absorbed doses from the methods varied within 2%. However, using the whole liver contour as the self-calibration region resulted in mean absorbed doses approximately 70% greater than the results when using a larger self-calibration region that included counts outside of the liver. Expanding or contracting the whole liver contour by 5 mm also had significant impacts on the absorbed dose results.[25]

In 2021, the European Association of Nuclear Medicine (EANM) dosimetry committee published recommendations for the standardization of 90Y absorbed dose calculations. They discussed using a patient-relative conversion method for activity quantification, which is equivalent to the LDM with Known Activity absorbed dose calculation. For the self-calibration region included in the conversion factor to convert PET or SPECT units to dose, they recommend using the total activity within the whole liver and lungs. In order to determine the total activity in the whole liver and lungs, it is recommended to acquire the complete structures in the field of view of the image.[26]

When using a larger self-calibration region, such as the entire PET or SPECT field of view, scatter and false counts outside of the liver can cause a significant underestimation of the absorbed doses within the liver. By restricting the self-calibration region to a smaller area where all of the injected activity is known to be, such as the whole liver or perfused volume, then counts that are not representative of true activity can be excluded from the normalization performed in the dose calculation. It is important to note that the accuracy of the contour used for the self-calibration region impacts the accuracy of the absorbed dose results. While using the entire PET or SPECT field of view as the self-calibration region may cause underestimation of the absorbed doses in the liver, using a smaller area as the self-calibration region introduces user-dependent error based on subjective contouring methods.

When using a smaller self-calibration region, any true activity that lies outside of the chosen contour must be accounted for. For example, if the lungs are not included in the self-calibration region, then the lung shunt value should be factored into the dose calculation to reduce the total injected activity in the liver. When using the lung shunt to accommodate for activity shunted out of the liver and into the lungs, the more quantitatively accurate 3D SPECT/CT lung shunt is preferred compared to the 2D lung shunt calculated from planar gamma camera imaging. Otherwise, using the 2D lung shunt value could cause underestimation of the absorbed doses in the liver.[26, 27] Additionally, if activity shunted elsewhere in the abdomen, then the self-calibration region should be adjusted to include

the volume containing the shunted activity. The self-calibration region can also be expanded by 1-2 cm to account for any true activity present outside of the boundary of the contour due to respiratory motion or resolution differences between the anatomical image and PET or SPECT.[28]

Multiple self-calibration regions can be defined using one PET or SPECT image to allow absorbed dose calculations to separate volumes that were selectively injected with 90Y during a single procedure. For example, if tumors located in different segments of the liver were treated by changing the catheter positioning and performing selective injections to each segment, then those separate volumes could be contoured and serve as separate self-calibration regions with different known injected activities for each region. The same considerations for contour accuracy and shunted activity apply in this case, but using multiple separate self-calibration regions allows for more accurate absorbed dose results in each treated volume compared to using a single self-calibration region with the total injected activity applied over the entire treated volume.

Effect of Image Modality System Resolution on ^{90}Y Dose

Phantom Creation

A simulated mathematical phantom was created by masking the voxel values of spherical ROIs to a known uniform ^{90}Y activity level. The spherical ROIs were 20, 30, 40, and 50 mm diameter in size. The image masking was done on an image with 0.5 mm voxel size and then the image was resampled to a 3x3x3 mm voxel size for the purpose of activity measurements. The spheres were convolved with 2, 4, 6, 8, 10, and 12 mm FWHM Gaussians to simulate the effect of PET/SPECT cameras with varying system resolution. A VSV dose was calculated as the gold standard dose by convolving the image volume that had no sphere smoothing (perfect image resolution) with the MIRD Pamphlet 17 ^{90}Y 3 mm voxel dose distribution matrix. This VSV dose represents a true dose distribution that includes deposition of ^{90}Y energy both in and beyond the source.

LDM ^{90}Y Dose Relative to PET System Resolution

The LDM dose calculation method was performed on each resolution phantom and mean dose values were recorded for each spherical ROI. The following graphs show the mean measured dose error in percent of the gold standard dose (VSV mean dose calculated from true activity distribution) as a function of system resolution for 20 and 50 mm diameter sphere sizes. Note that the y-axis is scaled differently for these 2 sphere sizes. A similar pattern was observed for sphere sizes 30 and 40 mm in diameter.

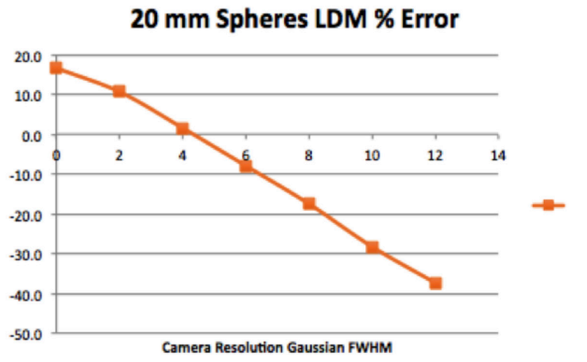

Figure 1

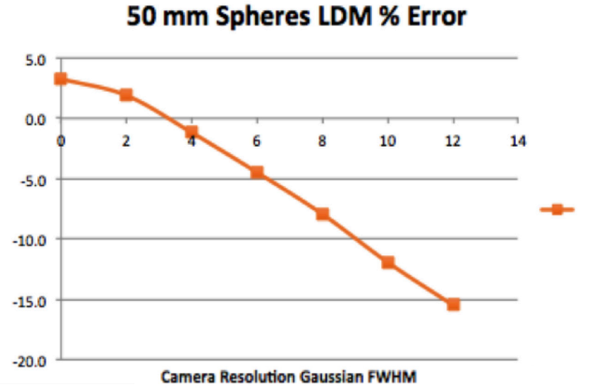

Figure 2

The effective ^{90}Y energy deposition resolution based on this study is approximately 4 mm FWHM since the error is nearly zero for this camera resolution. The difference in zero intercept for the two spheres is due to the non-Gaussian distribution of ^{90}Y energy as defined by the VSV matrix. For camera resolutions

less than 4 mm FWHM, camera measured activity spread beyond the spheres is less than the ^{90}Y energy spread beyond the spheres and therefore LDM dose measurements in the sphere are overestimated. Conversely, the dose is underestimated for resolutions greater than 4 mm FWHM. Fortunately for ^{90}Y LDM dose measurements, the resolution of PET/SPECT systems is generally in the 4 to 8 mm range.

Partial volume effect is caused by a finite camera resolution that causes some of the activity at a point to be added to the measured activity at adjacent points. Since ^{90}Y also has energy spread beyond a point source of ^{90}Y activity, we have shown in the previous graphs that a camera resolution similar to the energy spread of ^{90}Y has the least error for LDM dose measurements.

VSV Dose Relative to PET System Resolution

The same mathematical phantom described above for LDM was used to determine the effect of image resolution on VSV dose calculations. The following graphs show the mean measured VSV dose error in percent of the gold standard dose (VSV mean dose calculated from the true activity distribution) as a function of system resolution for 20 and 50 mm diameter sphere sizes. Note that the y-axis is scaled differently for these 2 sphere sizes. A similar pattern was observed for sphere sizes 30 and 40 mm in diameter.

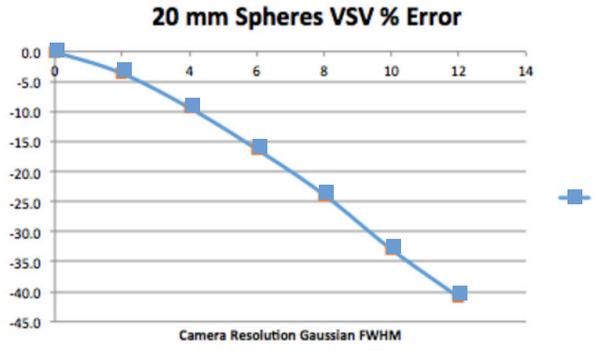

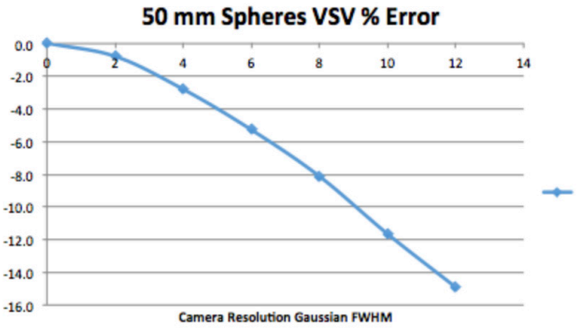

The VSV dose measurement depends on accurate measures of ^{90}Y activity and therefore error increases as the FWHM of the camera resolution increases. The error is due to reduced activity in the sphere region due to blurring of camera resolution, PVE, which moves activity outside the sphere to the background. The larger sphere has less error for any camera resolution relative to the smaller sphere. Background activity would add to activity measurements in the sphere and reduce the measured dose error. One advantage of the VSV method is that there is a measure of dose outside the object that is due to activity in the object.

A dose point kernel, DPK, has a smaller FWHM compared to VSV. As noted in MIRD Pamphlet 17, VSV is a better approximation for PET/SPECT imaging systems.

Influence of Voxel Size on LDM Dose Calculation

In order to evaluate the effect of voxel size, the simulated sphere phantom with a voxel size of 0.5 mm was interpolated to 2 mm, 3 mm, and 4 mm voxels using trilinear interpolation. All three images were smoothed with a 4 mm Gaussian to emulate the ideal PET resolution for LDM dose calculations. The following table shows the effect on mean counts in the spheres.

Table 1

4 mm smooth sphere diameter	2 mm voxels	Mean Counts 3 mm voxels	4 mm voxels (% change from 2 mm)
20 mm	312	302	292 (-6.4%)
30 mm	334	331	324 (-3.0%)
40 mm	347	343	341 (-1.7%)
50 mm	353	350	347 (-1.7%)

Table 1 Measured mean activity level in spheres from a phantom resampled to different voxel sizes

The VSV dose calculation method resamples the PET image voxels to a 3x3x3 mm matrix so the dose is always calculated on 3 mm voxels.

Image Resolution & Partial Volume Effect

The finite resolution of the imaging system can result in partial volume effect (PVE) whereby a resolution-based blurring of the imaging activity reduces the true activity in an object[29] and causes spillover of activity between regions. In essence, part of the signal from the source spills out of the actual source and is seen outside of the source. Objects that are small relative to the point-spread function (PSF) of the imaging system, expressed as the FWHM, have a reduced measured activity level due to PVE.

This effect can be modeled by convolving the 3D point-spread function (PSF) of the imaging system with the true activity distribution. To demonstrate the influence of PVE on image activity, a mathematical phantom was created by masking spherical regions to a known activity level and then progressively smoothing the image using a Gaussian filter with a FWHM from 2 mm to 12 mm at 2 mm increments. The spherical ROIs were 20, 30, 40, and 50 mm in diameter. The image masking was done on an image with a 0.5 mm voxel size and then the image was resampled to a 3x3x3 mm voxel size for the purpose of activity measurements. The images were resampled since images are interpolated to 3x3x3 mm resolution prior to convolution with the VSV (MIRD 17) dose distribution matrix. The mean activity level in each of the spherical ROIs was measured and compared to the known value. Results from this test can be seen in Table 2.

Table 2

Percent of True Activity (%)

Sphere Diameter	2 mm Smooth	4 mm Smooth	6 mm Smooth	8 mm Smooth	10 mm Smooth	12 mm Smooth
20 mm	88	80	72	65	56	49
30 mm	93	87	82	77	70	65
40 mm	94	90	86	82	77	73
50 mm	95	92	89	85	82	78

Table 2 Measured mean activity level in a sphere in % of the actual activity level following Gaussian smooth

Selection of Dose Measurement Method

All ^{90}Y PET and SPECT dose measurement methods are affected by image resolution and Beta minus particle energy spatial dose distribution. In the simulations depicted on p. 8 in Figures 1 and 2, LDM, which assumes that dose is proportional to measured activity within the source, overestimates dose for PET resolution FWHM less than 4 mm. For resolutions greater than 4 mm the dose is underestimated since the lower counts caused by the imaging system resolution, partial volume effect, are greater than the accumulation of dose due to the ^{90}Y spatial energy distribution. VSV dose measurement accuracy is ideal with perfect image resolution and continues to decrease as PET resolution worsens (increase in FWHM) due to greater blurring of the true activity distribution.

The LDM and LDM with Known Activity methods do not include the effect of dose from Bremsstrahlung radiation. The VSV method does include the effect of Bremsstrahlung dose, which is small within the source, compared to Beta minus energy as noted above. The 3 mm VSV dose deposition matrix has measures of

dose deposition for distances up to 18.75 cm from the source voxel. The LDM with Known Activity method is the only option when non-quantitative images, with count levels proportional to actual activity, are used for dose measurement. This method results in dose overestimation when all injected activity is not included in the field of view. Therefore, it is important to correct for the fraction of counts that are in the lung compared to the liver when the liver is treated as the whole field of view. In this way, the injected activity that is shunting outside of the liver is removed from the known activity scaling.

The average activity in the source would be the same for both LDM and VSV methods if the contour included regions outside the source with significant ^{90}Y energy deposition. When partial volume correction can be applied, the VSV method will give accurate source dose and also dose to target tissues. LDM dose will be overestimated for accurate PVC correction. LDM with Known Activity methods may be beneficial for low count PET images that affect PET quantitative accuracy by incorporating knowledge of the known injected activity.

References

1. Dezarn WA, Cessna JT, DeWerd LA, et al. Recommendations of the American Association of Physicists in Medicine on dosimetry, imaging, and quality assurance procedures for ^{90}Y microsphere brachytherapy in the treatment of hepatic malignancies. Med Phys (2011) 38(8).
2. SIR-Spheres(R) microspheres (Yttrium-90 Microspheres). Sirtex Medical Limited. November 2014 (CRI759). Accessed June 5, 2015. Available from: http://www.sirtex.com/media/29845/ssl-us-10.pdf
3. TheraSphere(R) Yttrium-90 Glass Microspheres Package Insert. BTG. Rev 12. Accessed June 5, 2015. Available from: http://www.therasphere.com/physicians-package-insert/TS_PackageInsert_USA_v12.pdf
4. Bolch WE, Bouchet LG, Robertson JS, et al. MIRD Pamphlet No. 17: The Dosimetry of Nonuniform Activity Distributions--Radionuclide S Values at the Voxel Level. J Nucl Med (1999), 40:11S-36S.
5. Nickles RJ, Roberts AD, Nye JA, et al. Assaying and PET imaging of yttrium-90. 2004; 3416:3412-3414.
6. Siman W, Mikell JK, Kappadath SC. Practical reconstruction protocol for quantitative ^{90}Y Bremsstrahlung SPECT/CT. Med Phys 2016; 43(9):5093-5103.
7. Lhommel R, van Elbmt L, Goffette P, et al. Feasibility of Y90 TOF PET-based dosimetry in liver metastasis therapy using SIR-Spheres. Eur J Nucl Med Mol Imaging 2010; 37:1654-1662.
8. Pasciak AS, Bourgeois AC, Bradley YC. A comparison of techniques for ^{90}Y PET/CT image-based dosimetry following radioembolization with resin microspheres. Frontiers in Oncology (2014) 4(121): 1-10.
9. Sanchez-Garcia M, Gardin I, Labtahi R, Dieudonne A. A new approach for dose calculation in targeted radionuclide therapy (TRT) based on collapsed cone superposition: validation with ^{90}Y. Phys Med Biol (2014) 59:4769-84.
10. Botta F, Mairani A, Hobbs RF, et al. Use of the FLUKA Monte Carlo dose for 3D patient specific dosimetry on PET-CT and SPECT-CT images. Phys Med Biol (2013) 58(22):8099-8120.

11. Dieudonne A, Hobbs RF, Lebtahi R, et al. Study of the Impact of Tissue Density Heterogeneities on 3-Dimensional Abdominal Dosimetry: Comparison Between Dose Kernel Convolution and Direct Monte Carlo Methods. J Nucl Med (2013), 54:236-243.
12. Selwyn RG, Nickles RJ, Thomadsen BR, DeWerd LA, Micka JA. A new internal pair production branching ratio of ^{90}Y: the development of a non-destructive assay for ^{90}Y and 90Sr. Appl Radiat Isot (2007) 65:318–27. doi:10.1016/j.apradiso.2006.08.009.
13. Willowson KP, Forwood N, Jakoby BW, et al. Quantitative Y90 image reconstruction in PET. Med Phys 2012; 39(11):7153-7159.
14. Willowson KP, Tapner M, The QUEST Investigator Team, Bailey D. A multicentre comparison of quantitative Y90 PET/CT for dosimetric purposes after radioembolization with resin microspheres. Eur J Nucl Med Mol Imaging 2015; 42:1202-1222.
15. Carlier T, Wilowson KP, Fourkal E et al. Y90-PET imaging: Exploring limitations and accuracy under conditions of low counts and high random fraction. Med Phys 2015; 42(7):4295-4309.
16. Srinivas SM, Natarajan N, Kuroiwa K, et al. Determination of radiation absorbed dose to primary liver tumors and normal liver tissue using post-radioembolization Y90 PET. Frontiers in Oncology 2014; 4(555):1-12.
17. Carlier T, Eugene T, Bodet-Milin C, et al. Assessment of acquisition protocols for routine imaging of Y90 using PET/CT. EJNMMI Research 2013;3:11.
18. Marti-Climent JM, Prieto E, Elosua C, et al. PET optimization and accurate quantification of Y90-microsphere biodistribution after radioembolization. Med Phys 2014; 41(9).
19. Rong X, Du Y, Ljungberg M et al. Development and evaluation of an improved quantitative Y90 Bremsstrahlung SPECT method. Med Phys 2012; 39(5):2346-2358.
20. Elschot M, Lam MGEH, van den Bosch MAAJ et al. Quantitative Monte Carlo-based Y90 SPECT reconstruction. J Nucl Med 2013; 54(9):1557-1563.
21. Dewarja Y, Roberson P, Clinthorne N et al. Quantitative Bremsstrahlung SPECT/CT image reconstruction with patient specific Monte Carlo scatter compensation for Y-90 microsphere radioembolization (RE). J Nucl Med 2012; 53 (Suppl 1):444.
22. Srinivas SM, Natarajan N, Kuroiwa J, et al. Determination of radiation absorbed dose to primary liver tumors and normal liver tissue using post-radioembolization ^{90}Y PET. Frontiers in Oncology (2014) 4(455).
23. Kao YH, Steinberg JD, Tay YS et al. Post-radioembolization yttrium-90 PET/CT - part 2: dose-response and tumor predictive dosimetry for resin microspheres. EJNMMI Research 2013; 3:57.
24. Stabin MG. Eckerman KF, Ryman JC, Williams LE. Bremsstrahlung Radiation Dose in Yttrium-90 Therapy Applications. J Nucl Med (1994) 35:1377-1380.
25. Balagopal A, Kappadath SC. Characterization of 90 Y-SPECT/CT self-calibration approaches on the quantification of voxel-level absorbed doses following 90 Y-microsphere selective internal radiation therapy. Med Phys 2018; 45(2):875-883.
26. Chiesa C, Sjogreen-Gleisner K, Walrand S, et al. EANM dosimetry committee series on standard operational procedures: a unified methodology for 99mTc-MAA pre- and 90Y peri-therapy dosimetry in liver radioembolization with 90Y microspheres. EJNMMI Physics 2021; 8(77).
27. Allred JD, Niedbala J, Mikell JK, et al. The value of 99mTc-MAA SPECT/CT for lung shunt estimation in 90Y radioembolization: a phantom and patient study. EJNMMI Res 2018; 8(50)
28. Thompson BC, Dezarn WA. Retrospective SPECT/CT dosimetry following transarterial radioembolization. J Appl Clin Med Phys 2021; 22(4):143-150.
29. Soret M, Bacharach SL, Buvat I. Partial-Volume Effect in PET Tumor Imaging. J Nucl Med 2007; 48:932-945. DOI: 10.2967/jnumed.106.035774.